sEEG is a Safe Procedure for a Comprehensive Anatomic Exploration of the Insula: A Retrospective Study of 108 Procedures Representing 254 Transopercular Insular Electrodes

Anne Laure Salado, MD*
Laurent Koessler, PhD‡§¶
Gabriel De Mijolla, MD#
Emmanuelle Schmitt, MD||
Jean-Pierre Vignal, MD‡§¶
Thierry Civit, MD¶#
Louise Tyvaert, MD, PhD‡§¶
Jacques Jonas, MD, PhD‡§¶
Louis Georges Maillard, MD, PhD‡§¶
Sophie Colnat- Coulbois, MD, PhD#

*Neurosurgery Department, University Hospital of Liège, Liège, Belgium; ‡CNRS CRAN UMR 7039, Vandœuvre-lès-Nancy, France; §Université de Lorraine, CRAN, UMR 7039, Vandœuvre-lès-Nancy, France; ¶Neurosurgery Department, University Hospital of Nancy, Nancy, France; #Neurosurgery Department, University Hospital of Nancy, Nancy, France; ||Neuroradiology Department, University Hospital of Nancy, Nancy, France

Correspondence:
Sophie Colnat-Coulbois, MD, PhD,
Service de Neurochirurgie,
Hôpital Central,
27 avenue du Maréchal de Lattre de Tassigny,
54000 Nancy, France.
E-mail: sophie.colnat@wanadoo.fr

Received, July 14, 2016.
Accepted, April 3, 2017.

BACKGROUND: The exploration of the insula in pre-surgical evaluation of epilepsy is considered to be associated with a high vascular risk resulting in an incomplete exploration of the insular cortex.

OBJECTIVE: To report a retrospective observational study of insular exploration using stereoelectroencephalography (sEEG) with transopercular and parasagittal oblique intracerebral electrodes from January 2008 to January 2016. The first purpose of this study was to evaluate the surgical risks of insular cortex sEEG exploration. The second purpose was to define the ability of placing intracerebral contacts in the whole insular cortex.

METHODS: Ninety-nine patients underwent 108 magnetic resonance imaging (MRI)-guided stereotactic implantations of intracerebral electrodes in the context of preoperative assessment of drug-resistant epilepsy, including at least 1 electrode placed in the insular cortex. On postoperative computed tomography images co-registered with MRI, followed by MRI segmentation and application of a transformation matrix, intracerebral contact coordinates of the insular electrodes' contacts were anatomically localized in the Talairach space. Finally, dispersion and clustering analysis was performed.

RESULTS: There was no morbidity, in particular hemorrhagic complications, or mortality related to insular electrodes. Statistical comparison of intracerebral contact positions demonstrated that whole insula exploration is possible on the left and right sides. In addition, the clustering analysis showed the homogeneous distribution of the electrodes within the insular cortex.

CONCLUSION: In the presurgical evaluation of drug-resistant epilepsy, the insular cortex can be explored safely and comprehensively using transopercular sEEG electrodes. Parasagittal oblique trajectories may also be associated to achieve an optimal exploration.

KEY WORDS: Complications, Depth electrodes, Epilepsy surgery, Insula, Neuroimaging, SEEG (stereoelectroencephalography), Stereotactic procedure

Operative Neurosurgery 0:1–8, 2017 DOI: 10.1093/ons/opx106

Early in the 1950s, Guillaume and Mazars[1] in France and Penfield and Faulk[2] in Canada pointed out the involvement of the insular lobe in drug-resistant epilepsy and reported resection of insular cortex. More recently, Isnard et al,[3] using stereoelectroencephalography[4] (sEEG), studied the clinical manifestations of insular lobe seizures. They also demonstrated the involvement of insula in temporal lobe epilepsy.[5] Gras-Combes et al[6] showed that insular resection based on sEEG findings can be performed safely with a significant chance of seizure freedom. The anatomic localization of insular cortex is particularly challenging for presurgical evaluation of epilepsy, as it is covered by the frontal, parietal, and temporal opercula in the depths of the sylvian fissure.[7] Furthermore, the vicinity of middle

ABBREVIATIONS: CSF, cerebrospinal fluid; **EEG,** electroencephalographic; **MRI,** magnetic resonance imaging; **PET,** positron emission tomography; **sEEG,** stereoelectroencephalography; **3-D,** 3-dimensional

Supplemental digital content is available for this article at (www.operativeneurosurgery-online.com).

cerebral arteries branches potentially increases the risk of hemorrhagic complications following invasive recordings. Thus, the insula has long been considered to be inaccessible to intracerebral explorations.[8] However, more recently, several publications have reported insular exploration using sEEG[3,9-11] or a combination of subdural grids and intracerebral electrodes.[12] For sEEG, vascular risk has been associated with transopercular trajectories, and the oblique parasagittal electrodes have been considered safer.[9,11]

Here, we report our experience of sEEG insular exploration in 108 procedures, representing 261 electrodes, with both transopercular and oblique trajectories. The first purpose of this study was to define the surgical risk of insular cortex sEEG exploration. The second purpose was to define the possibility of placing intracerebral contacts into the whole insular cortex. To the best of our knowledge, this is the largest series of insular explorations reported in the literature.

METHODS

Participants

We retrospectively analyzed 144 consecutives sEEG procedures for evaluation of drug-resistant epilepsy performed between January 2008 and January 2016 in the University Hospital of Nancy.

In all cases, noninvasive presurgical evaluation included: high-resolution electroencephalographic (EEG) video monitoring combined to electrical source imaging analysis,[13] neuropsychological tests, axial diffusion, and positron emission tomography (PET), high-resolution magnetic resonance imaging (MRI) with coronal 3-dimensional (3-D) T1 FSPGR high-resolution-weighted images, axial T2* weighted images, coronal T2 FSEIR and sagittal 3-D FLAIR MRI. Intracerebral exploration was decided when this evaluation leaded to a strong suspicion of a unique epileptogenic zone. Implantation planning was then used to delimitate the epileptogenic zone and, if necessary, provide functional mapping. The inclusion criterion in this study was the presence of at least one electrode in the insular cortex. Despite the retrospective character of the study, there was no selection bias since all eligible consecutive patients were enrolled in the study and there was no loss to follow up. All patients gave their informed consent to participate in this study in accordance with the university hospital ethic committee.

Surgical Procedure

Implantation Planning

A few days before surgery, patients underwent nonstereotactic MRI (Axial strict 3-D SPGR T1 weighted-sequence, thickness 1.2 mm, 20/6/1 (TR/TE/excitation), 256 × 256 display matrix, FOV, 280 × 210 mm. Signa Twin Speed HDxt, 1.5T, General Electric Medical Systems Milwaukee, Wisconsin) with double injection of gadolinium (Multihance®, gadobenate dimeglumine, 0.5 mmol/mL): bolus before the acquisition (10 mL) and continuous perfusion during the acquisition time (10 mL in 50 mL of 0.9% sodium chloride). Implantation planning was designed by the neurosurgeon (SCC) and the neurologist (LM, JPV, LT) using the Iplanstereotaxy® software (Brainlab AG, Feldkirchen, Germany). The implantation scheme was defined individually for each patient according to electro-clinical hypothesis derived from noninvasive investigation. The general pattern was the following: when the main hypothesis was temporoinsular, it comprised 2 infrasylvian transopercular trajectory and 2 or 3 suprasylvian trajectories. When the main hypothesis was insuloperisylvian, it comprised 3 infra- and 3 suprasylvian plus anterior and posterior oblique. When the hypothesis was insulofrontal, it generally comprised 2 transopercular frontal and 1 transopercular temporal. We respected a safety margin of 2 mm between the trajectory and the nearby vessels.

Electrode Implantation

After induction of general anesthesia, the stereotactic frame (Leksell model G, Elekta instrument, Stockholm, Sweden) was positioned on patient's head. A stereotactic CT-scan was then performed and fused to the preoperative nonstereotactic MRI using the Iplanstereotaxy® software (Brainlab AG). Electrodes were then implanted according to the following procedure: after reporting the calculated coordinates on the frame, stereotactic guided drilling of the skull was performed and a bone screw was inserted. The intracerebral electrode (Dixi Medical, Besançon, France, diameter of 0.8 mm; 5 to 18 Platinum/Iridium contacts with, 2 mm length, 1.5 mm apart) was inserted and secured to the screw with a tight seal in order to prevent cerebrospinal fluid (CSF) leak. Fluoroscopic control was performed to rule out major electrode positioning errors before removing the stereotactic frame.

Postoperative Assessment

Patient systematically underwent postoperative CT-scan to check for potential surgical complications and to determine the anatomic position of each contact of each electrode using fusion with the preoperative MRI (Figures 1A-1E). For 5 to 10 days, video-EEG-SEEG[14] was continuously recorded. Afterwards, the electrodes were removed under local anesthesia. Patients underwent a full clinical assessment immediately after implantation, every day during sEEG recordings, at day 1, 3, and 60 after electrode removal.

Data Measurement: Anatomic Study of the Position of Insular Contacts

Anatomy of Insular Lobe

We used the nomenclature proposed by Tanriover et al[7] to describe the anatomy of the insular region. The insula is a pyramid-shaped lobe, covered by frontal, temporal, and parietal opercula, on the floor of the sylvian fissure. The circular sulcus defined the external limits of the insula. The central insular sulcus divides the insula into 2 portions, anterior and posterior. The anterior insula is composed of the 3 short insular gyri (anterior, middle, posterior) and 2 other less important: accessory and transverse insular gyri. All 5 gyri converge at the insular apex, which represents the most superficial aspect of the insula. The insular apex is the highest and most prominent laterally projecting area on the insular convexity. The posterior insula is composed of the anterior and posterior long insular gyri. The pole of the posterior lobule indicated the most anterior extent of the posterior lobule of the insula where the 2 long gyri converge to form the posterior wall of the limen insula.

In this study, we defined 3 regions of interest: the anterior region that corresponded to the short gyri, the posterior region that corresponded to the long gyri, and the apex region including the apex insula, the anterior and posterior pole of insula (Figure 2).

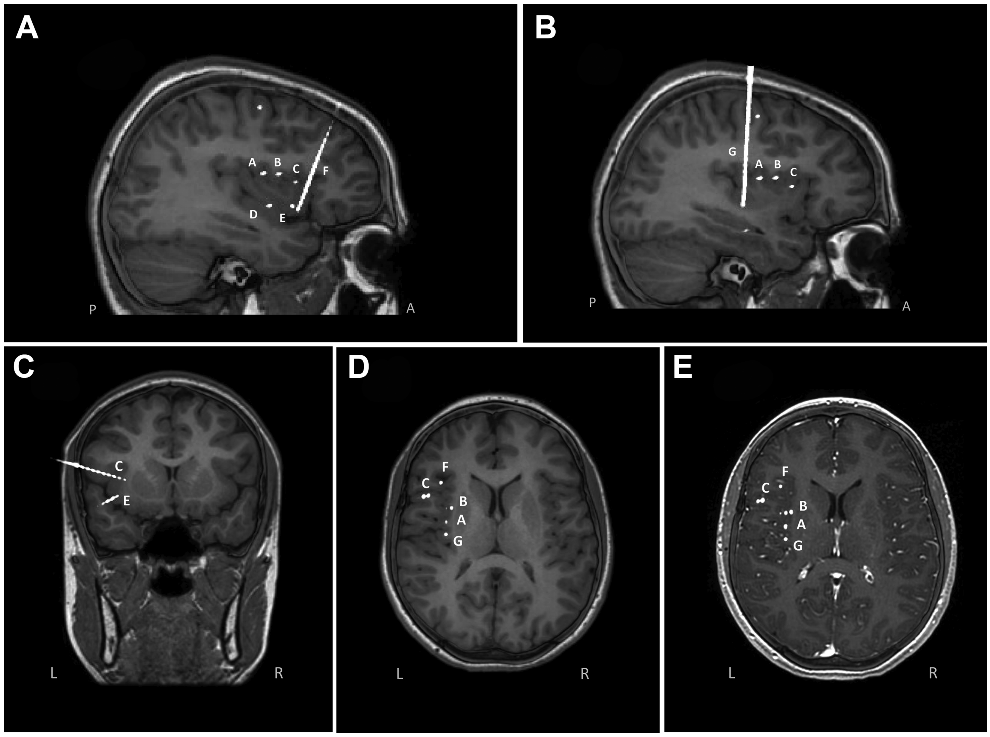

FIGURE 1. **A**, *Insular exploration in a patient with insular epilepsy: postoperative CT-scan fused with preoperative MRI (T1 weighted images without injection of gadolinium). Sagittal view. A,B,C = frontal trans-opercular insular electrodes. D,E = temporal trans-opercular insular electrodes. F = transfrontal oblique anterior insular electrode.* **B**, *Insular exploration in the same patient: postoperative CT-scan fused with preoperative MRI (T1 weighted images without injection of gadolinium). Sagittal view 3 mm medially to Figure 1A. A,B,C = frontal trans-opercular insular electrodes. G = transfrontal oblique posterior insular electrode. D and E are not visible because the plan section passes between 2 contacts. In the same way, F is located more laterally and cannot be visualized.* **C**, *Insular exploration in the same patient: postoperative CT-scan fused with preoperative MRI (T1 weighted images without injection of gadolinium). Frontal view. Visualization of electrodes C and E.* **D**, *Insular exploration in the same patient: postoperative CT-scan fused with preoperative MRI (T1 weighted images without injection of gadolinium). Axial view. Visualization of electrodes F, C, B, A, and G.* **E**, *Insular exploration in the same patient: postoperative CT-scan fused with preoperative MRI (T1 weighted images with double injection of gadolinium). Axial view. Visualization of electrodes F, C, B, A, and G.*

Tridimensional Localization of Intracerebral Electrodes

The intracerebral electrodes in the head volume were detected and localized in three steps: detection of intracerebral electrodes in CT scan; co-registration of CT and preoperative MRI by calculating a transformation matrix; and finally brain tissue segmentation in MR images.[15]

Detection of intracerebral electrodes in CT scan relied on the following.

(1) Skull stripping using intensity level thresholding and image morphological processing methods to segment intracranial space where intracerebral electrodes are placed.
(2) Correlation of the pattern (CT artifacts) using a 3-D correlation to segment the intracranial volume (see step 1) with a simulated pattern which is an approximation of intracerebral electrode (length of the contact, intercontact distance, diameter; DIXI electrode).
(3) Identification of the multicaptor that correctly interprets the local maxima of the 3-D correlation in the CT images. This method analyses given local maximums points, detects all sets of points corresponding to the intracerebral contacts and eliminates all other points.

CT and MR images were co-registered using voxel-based registration (SPM 8 toolbow for Matlab; Mathworks, Natick, Massachusetts), where the optimization criterion was directly calculated from the voxels intensity levels. We chose the approach based on mutual information maximization[16-18] that is widely used in multimodality image registration[19-21] and that presents an accuracy better than 1 mm.[22] Finally, intracerebral electrode positions were labeled with respect to brain matter using MR segmentation using the surface-based pipeline method[23,24] introduced in FreeSurfer (Martinos Center for Biomedical Imaging, Harvard, Cambridge, Massachusetts). For each patient, anatomic landmarks (anterior commissure, posterior commissure, interhemispheric point, anterior point, posterior point, right point, left point, inferior point, posterior point) were manually positioned by a trained

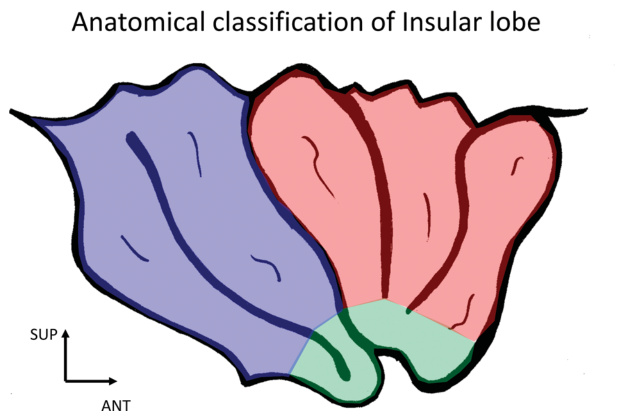

FIGURE 2. *Schematic representation of insular anatomy and determination of 3 main regions: the anterior region (red) that corresponded to the short gyri, the posterior region (blue) that corresponded to the long gyri, and the apex region (green) including the apex insula and the anterior and posterior pole of insula.*

expert (AS) on the individual MR images. A transformation matrix was applied to obtain intracerebral contact coordinates in the Talairach space. Then, all intracerebral contacts in the Talairach space from all patients were merged and finally displayed in a normalized MR Template (Colin 27[25]). For 3-D visualization, Colin 27 average brain was segmented in SPM8 and the pial surface was depicted using the surface extraction procedure.

Quantitative Variables: Dispersion Analysis and Automatic Clustering Analysis of Intracerebral Contacts

First, center of gravity positions were calculated for left and right insula. Using centers of gravity, intracerebral contact coordinates were classified according to anterior inferior, anterior superior, posterior inferior, or posterior superior positions. Then, standard deviations in the 3 space directions and box plots were calculated for both insulae. Finally, automatic clustering analysis (K-means) was used to define, independently of the operator, the numbers and positions of intracerebral contact clusters in both insulae. Two to 6 classes were used for clustering. Mean values of silhouette (Euclidean distance) were calculated and used to measure of how similar an intracerebral contact position is to its own cluster compared to other clusters.

RESULTS

Population

Among the total of 144 sEEG procedures representing 130 patients, we found 108 procedures (99 patients) meeting the inclusion criterion. There were 44 women and 55 men (mean age 30 yr old (ranges 8-53 yr old). Thirty patients had a normal cerebral MRI against 69 patients who have abnormal cerebral MRI (including 6 patients with insular lesion). Prior to sEEG implantation, the insular cortex was suspected to be primarily involved in 72 patients and secondarily involved in 27 patients. sEEG demonstrated primary involvement of insular cortex in 41 procedures, secondary involvement in 22 procedures and no involvement in 45 procedures. Final therapeutic decisions included insular or extra-insular cortex resection, radiofrequency thermocoagulation or contraindication (Table).

Descriptive Data

sEEG implantation was unilateral in 36 procedures and bilateral in 72. These 108 procedures represent a total of 1292 intracerebral electrodes (mean 12 electrodes/patients, [7-18]) among whom 261 were in the insular cortex (mean 2 insular electrodes/patients, [1-7]). The chosen trajectory was transopercular perpendicular to the sagittal plane for 254 electrodes and oblique with transfrontal or transparietal approach for 7 electrodes. Given the small number of oblique electrodes, we excluded them from the statistical analysis.

In total, the insular cortex was explored by 254 electrodes representing 458 contacts (mean 4.2 ± 2.9 insular contact/patient, max 16 contacts/patient [1-23]).

Outcome Data

No morbidity or mortality was associated to insular trajectories. Considering the totality of the 1292 intracerebral implanted electrodes, 7 hemorrhages were diagnosed including 1 epidural hematoma that required surgical evacuation. There was

TABLE. Therapeutic decision according to the findings of the 108 sEEG procedures

		sEEG findings (n = 108 proc.)			
		I (n = 41 proc.)	II (n = 22 proc.)	No (n = 45 proc.)	Total
Therapeutic decision	Insular cortectomy alone	1	0	0	1 **(0.9%)**
	Insular cortectomy + Insular RF-thermocoagulation	5	0	0	5 **(4.6%)**
	Insular RF-thermocoagulation alone	7	0	0	7 **(6.5%)**
	Extra-insular cortectomy	6	17	33	56 **(51.9%)**
	Extra-insular cortectomy + Insular RF-thermocoagulation	7	1	0	8 **(7.4%)**
	Contraindication	15	4	12	31 **(28.7%)**

Legend: I = primary insular involvement; II = secondary insular involvement; No = no insular involvement; proc. = procedures; RF = radiofrequency.
Percentage in bold represents the ratio between the number of therapeutic decisions and all sEEG procedures (n = 108)

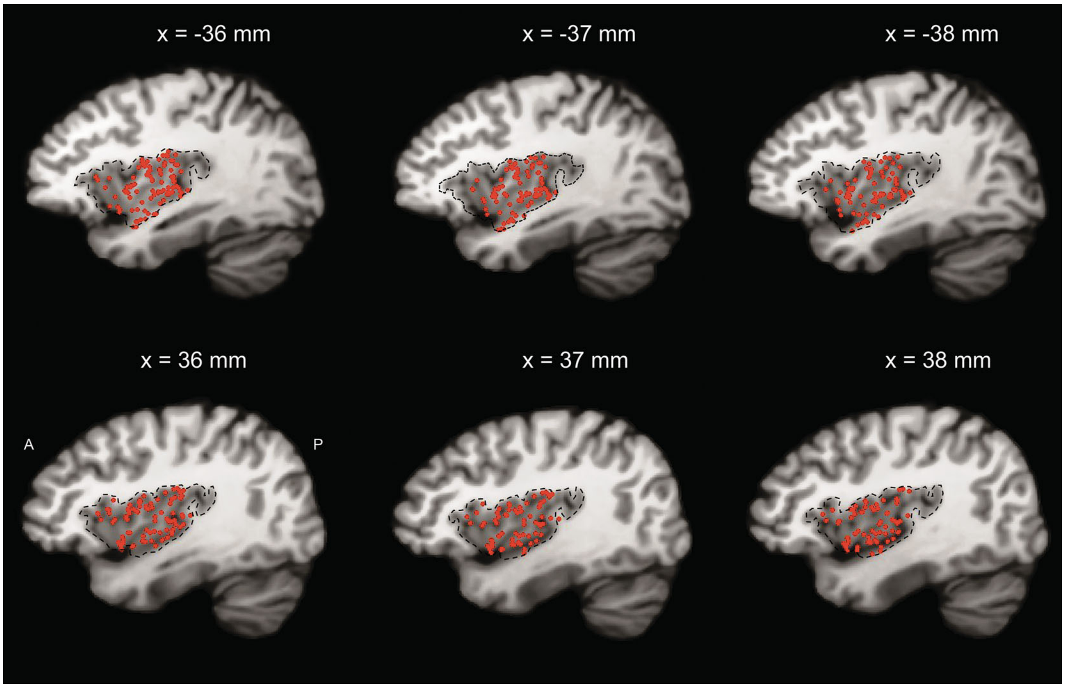

FIGURE 3. *Selection of sagittal views of the insula (black dotted lines) on the left (upper row) and right (lower row) insula (black dot lines) with all intracerebral contacts (red dots) from 254 insular electrodes in a Colin 27 anatomic MRI.*

1 subarachnoid hemorrhage, 2 frontal hematomas, and 3 temporal hematomas with only 1 responsible of mild transient dysphasia. We found 1 intracranial screw migration during implantation procedure and 4 fractures of electrode following seizures. No infection was reported. Finally, 1 patient had a pneumocephalus with transient motor deficit after electrodes removal.

Main Results

Anatomic Localization of Insular Contacts

Among the 458 insular contacts, 198 were localized in the anterior region, 207 in the posterior region, and 53 in the apex (Figure 3). On average, 1.8 ± 2.1 contacts were in the anterior region, 1.9 ± 1.8 in the posterior and 0.5 ± 1 in the apex. In right insula investigations (234 contacts), we classified 50 intracerebral contacts as antero-inferior, 73 anterosuperior, 59 postero-inferior, and 52 posterosuperior. In left insula investigations (224 contacts), we classified 56 intracerebral contacts as antero-inferior, 50 anterosuperior, 45 postero-inferior, and 73 posterosuperior.

Dispersion and Automatic Clustering of Left and Right Insula

Standard deviation in the right insula was 3.8 mm in the x-axis, 12.5 mm in the y-axis and 8 mm in the z-axis. Standard deviation in left insula was 3.8 mm in the x-axis, 13.6 mm in the y-axis, and 8.8 mm in the z-axis (Figure 4). Distance between the outermost points in the left insula was 19.4 mm in x, 58.6 mm in y, and 36.7 mm in z. Distance between the outermost points in right insula was 17.9 mm in x, 49.5 mm in y, and 31.8 mm in z. Automatic clustering showed, respectively, 3 and 5 different clusters in the left and the right insula. These numbers of clusters corresponded to the higher silhouette values: 0.642 for 3 clusters in the left insula (compared to 0.319, 0.575, 0.589, 0.585 for 2, 4, 5, and 6 clusters) and 0.630 for 5 clusters in the right insula (compared to 0.597, 0.614, 0.618, 0.620 for 2, 3, 4, and 6 clusters; Figure 5). For the 3 clusters configuration, 43, 65, and 116 intracerebral contacts were found in the left insula and 62, 83, and 89 in the right insula. For the 5 clusters configuration, 38, 42, 43, 47, 54 intracerebral contacts were found in the left insula and 36, 45, 48, 51, 54 in the right insula.

DISCUSSION

Key Results

There was no morbidity, in particular hemorrhagic complications, or mortality related to insular electrodes. Statistical comparison of intracerebral contact positions demonstrated that whole insula exploration is possible on the left and right sides. In addition, the clustering analysis showed the homogeneous distribution of the electrodes within the insular cortex.

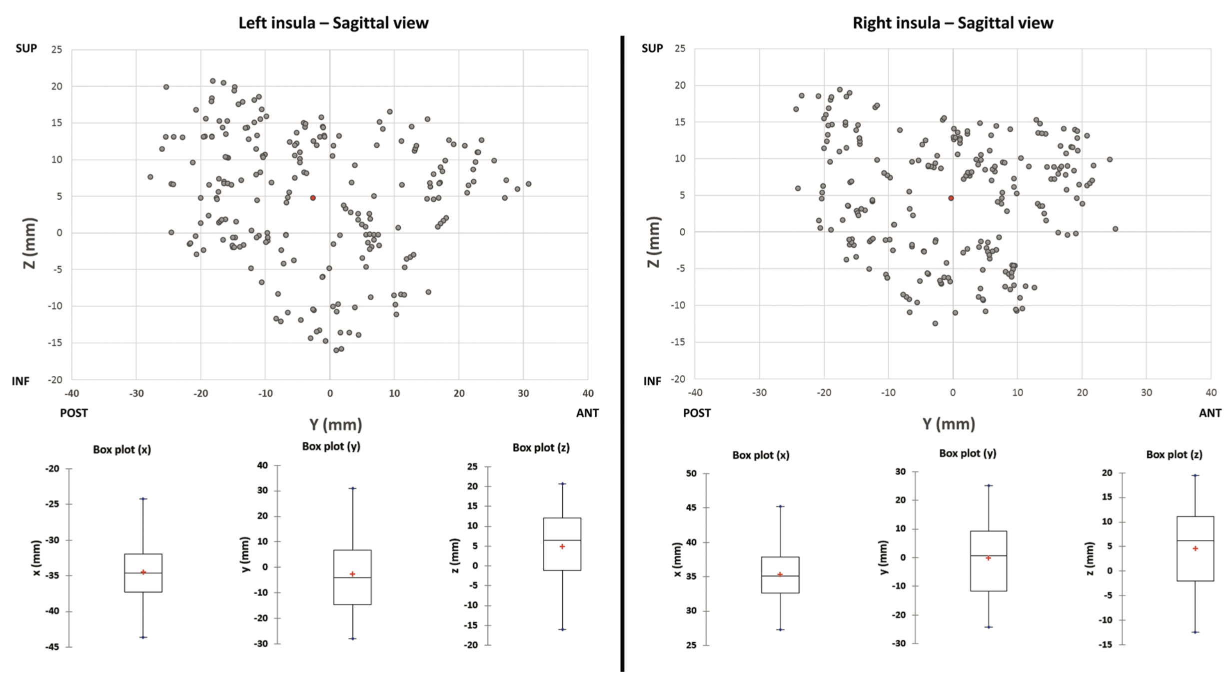

FIGURE 4. *Upper part: Plane projection of all intracerebral contacts in sagittal views (left insula on the left and right insula on the right). The red dots correspond to the barycenter positions; lower part: box plots in x-, y-, and z-axis that give an over view of the intracerebral contact distributions in the insular lobes.*

Interpretation and Generalizability

Safety of Insular Exploration with sEEG

sEEG is associated with postoperative complications, the most feared being intracranial hemorrhage. Its frequency is well reported in the literature, ranging from 0% to 3.7%.[10,26-31] In this series, none of the hemorrhagic complications (0.7%) was found on the trajectory of the insular electrodes, despite the known high vascular density of the area. Some authors emphasized the vascular risk[9,11] theoretically associated with transopercular trajectories and thus proposed that oblique trajectories may be safer. However, there are no data in the literature that demonstrate this perceived higher risk with transopercular trajectories. The group of Lyon, France, who published about insular sEEG explorations with this approach early, did not mention any hemorrhagic complications specifically related to insular electrodes.[3] Robles et al[9] raised the issue of a theoretical risk of the transopercular approach in dominant side. In our experience, however, we never observed any functional disturbance in eloquent area attributable to the presence of opercular electrodes, which on the other hand provided precious functional data when stimulating the cortex.

We mainly used the transopercular trajectory for several reasons. First, it allows sampling both the opercular and the insular cortex. This is of crucial importance for the interpretation of the seizure and its propagation,[10] particularly in temporal lobe epilepsy in which insular involvement is often demonstrated.[32] Second, transopercular trajectories are in most cases orthogonal to the skull, making the drilling safer, with, in our experience, a lower risk of electrode deviation. Finally, when considering the potential surgical resection for the patient, who is delimited by the sEEG electrodes, it is much easier to imagine a volume of resection lined by orthogonal planes than by oblique planes. In addition, we believe that the double injection of gadolinium on pre-operative MRI provides excellent visualization of vascular structures (Figure 1E), and the trajectory can be safely planned accordingly.

There are not any technical limitations related to the use of a stereotactic frame, as the Leksell G frame allows achieving both orthogonal and oblique trajectories. Therefore, we also used parasagittal oblique trajectories mainly to achieve an optimal insular exploration in case of pure insular epilepsy, always in association with transopercular electrodes. As Afif et al[11] have demonstrated, oblique trajectories are particularly useful for large sampling of insular cortex. In our experience, they are, however, also associated with certain difficulties. First, the insular cortex is often not strictly localized in a pure sagittal plane but in an oblique plane, so that the entry point of the electrode can approach midline venous structures. Second, the insular cortex is very thin and can be missed in case of electrode deviation. Third, in our experience, oblique drilling is associated with higher risk of deviation. We are nevertheless convinced that these

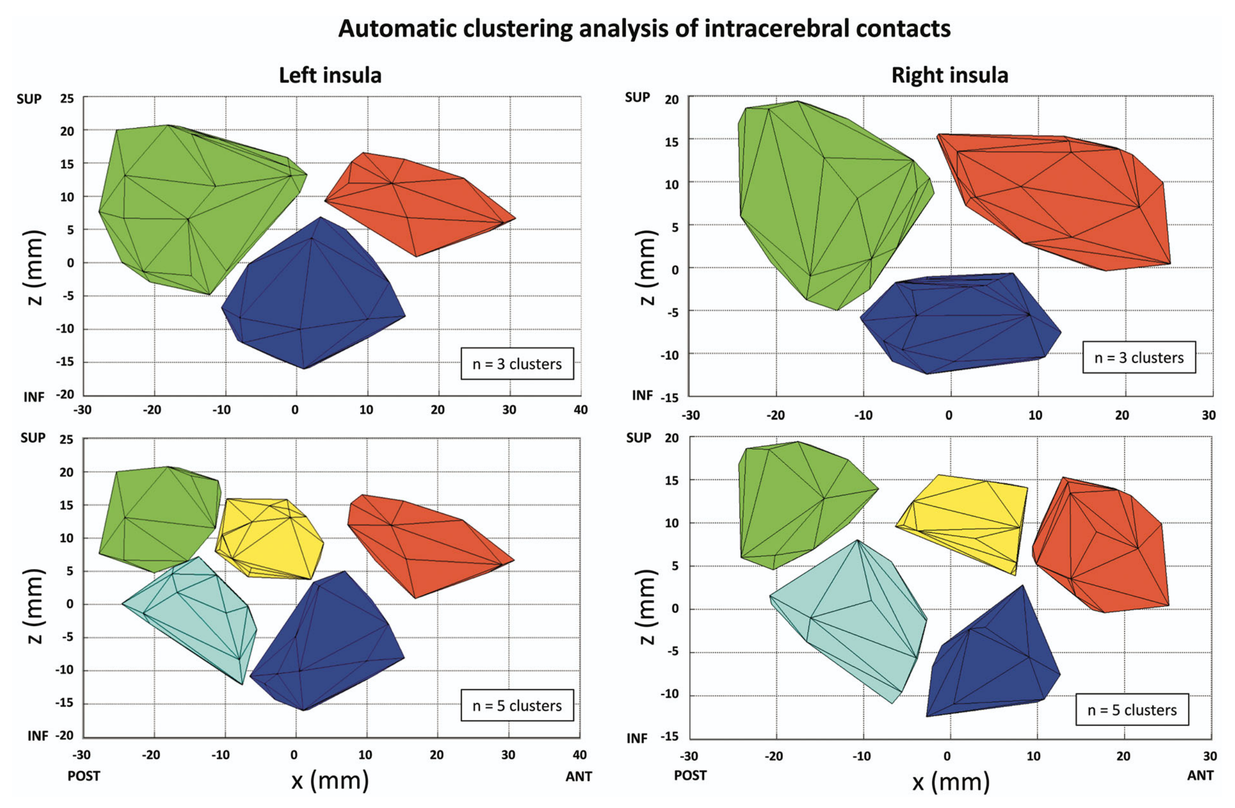

FIGURE 5. *Clustering analysis of left and right insula. On the upper row: the depicted 3 clusters are showing and are corresponding to the insular anatomic classification we defined: anterior (red), posterior (blue), and apex (green). Mean silhouette values were 0.642 for left insula and 0.614 for right insula. On the lower row: The 5 clusters are showing. This configuration is quite similar to the 3 clusters cluster-configuration, with only the posterior region being subdivided into 3 clusters (blue, yellow, and cyan). Mean silhouette value was 0.589 for left insula and 0.630 for right insula.*

2 complimentary approaches are useful and should both be used for a comprehensive exploration of insula. More invasive methods, requiring open craniotomy, for insular exploration, using a combination of subdural grids and depth electrodes[12,33] are based on a fundamentally different concept of intracerebral exploration and surgical strategy, associated with significant morbidity. Even though there may be benefits, the higher ratio of risk to benefice has kept our team from considering that strategy.

Comprehensive Exploration of Insular Cortex

Our study demonstrates that sEEG can provide a comprehensive exploration of the insular cortex. The long distance between the outermost intracerebral contact positions, combined with the large dispersions in the y- and z-axis demonstrate the possibility of exploring the insular cortex very widely. Quantitative comparison of intracerebral contact positions demonstrates that a comprehensive exploration of the insula is possible in left and right sides. The most difficult region to explore was the midpoint of the insula ($y = 0$ mm; $z = 0$ mm), where middle cerebral arteries branches are located. Automatic clustering demonstrates that, regardless of the clinicians, intracerebral contact clusters fit to our anatomic classification with the short gyri (anterior cluster, Figure 5; red cluster), the long gyri (posterior cluster[s], Figure 5: green cluster for $n = 3$ and green, yellow, and cyan clusters for n = 5) and the apex (antero-inferior cluster, Figure 5: blue cluster). Some authors reported that orthogonal transopercular approach does not permit access to the whole insula.[10,11] We demonstrate that the transopercular approach does allow for a comprehensive study of the insular cortex.

Limitations

Despite the retrospective character of the study, there was no selection bias since all eligible patients were enrolled in the study and there was no loss to follow-up. Furthermore, we consider that the small number of oblique electrodes reported in our study does not allow us to conclude about the specific risk associated to these trajectories.

CONCLUSION

The insular cortex can be explored safely and comprehensively using transopercular sEEG electrodes. Those trajectories also allow achieving an optimal exploration of the opercular cortex, which is crucial for the understanding of the seizure pattern and for the cortical functional mapping. The quality of this preoperative exploration is of tremendous importance for the success of the potential subsequent cortical resection.

Disclosures

Dr Salado received a grant from the University Hospital of Liège, Belgium. The authors have no personal, financial, or institutional interest in any of the drugs, materials, or devices described in this article.

REFERENCES

1. Guillaume J, Mazars G. [Technics of resection of the insula in insular epilepsies]. *Rev Neurol.* 1949;81(10):900-903.
2. Penfield W, Faulk ME. The insula; further observations on its function. *Brain J Neurol.* 1955;78(4):445-470.
3. Isnard J, Guénot M, Sindou M, Mauguière F. Clinical manifestations of insular lobe seizures: a stereo-electroencephalographic study. *Epilepsia*. 2004;45(9):1079-1090.
4. Talairach J, Bancaud J. Stereotaxic approach to epilepsy. Methodology of anatomo-functional stereotaxic investigations. *Prog Neurol Surg*. 1973;5:297-354.
5. Isnard J, Guénot M, Ostrowsky K, Sindou M, Mauguière F. The role of the insular cortex in temporal lobe epilepsy. *Ann Neurol*. 2000;48(4):614-623.
6. Gras-Combe G, Minotti L, Hoffmann D, Krainik A, Kahane P, Chabardes S. Surgery for nontumoral insular epilepsy explored by stereoelectroencephalography. *Neurosurgery*. 2016;79(4):578-588.
7. Tanriover N, Rhoton AL, Kawashima M, Ulm AJ, Yasuda A. Microsurgical anatomy of the insula and the sylvian fissure. *J Neurosurg*. 2004;100(5):891-922.
8. Bancaud J, Dell MB. [Technics and method of stereotaxic functional exploration of the brain structures in man (cortex, subcortex, central gray nuclei)]. *Rev Neurol*. 1959;101:213-227.
9. Robles SG, Gelisse P, El Fertit H, et al. Parasagittal transinsular electrodes for stereo-EEG in temporal and insular lobe epilepsies. *Stereotact Funct Neurosurg*. 2009;87(6):368-378.
10. Dylgjeri S, Taussig D, Chipaux M, et al. Insular and insulo-opercular epilepsy in childhood: an SEEG study. *Seizure*. 2014;23(4):300-308.
11. Afif A, Chabardes S, Minotti L, Kahane P, Hoffmann D. Safety and usefulness of insular depth electrodes implanted via an oblique approach in patients with epilepsy. *Neurosurgery*. 2008;62(5 suppl 2):ONS471-ONS479; discussion 479-480.
12. Surbeck W, Bouthillier A, Weil AG, et al. The combination of subdural and depth electrodes for intracranial EEG investigation of suspected insular (perisylvian) epilepsy. *Epilepsia*. 2011;52(3):458-466.
13. Rikir E, Koessler L, Gavaret M, et al. Electrical source imaging in cortical malformation-related epilepsy: a prospective EEG-SEEG concordance study. *Epilepsia*. 2014;55(6):918-932.
14. Koessler L, Cecchin T, Colnat-Coulbois S, et al. Catching the invisible: mesial temporal source contribution to simultaneous EEG and SEEG recordings. *Brain Topogr*. 2015;28(1):5-20.
15. Hofmanis J, Louis-Dorr V, Caspary O, Maillard L. Automatic depth electrode localization in intracranial space. *4th International Conference on Bio-inspired Systems and Signal Processing, Biosignals 2011*, Jan 2011; Rome, Italy, pp. :459-462.
16. Collignon A, Maes F, Delaere D, Vandermeulen D, Suetens P, Marchal G. Automated multi-modality image registration based on information theory. *Inform. Process. Med. Imaging*. 1995; 3:263-274.
17. Maes F, Collignon A, Vandermeulen D, Marchal G, Suetens P. Multimodality image registration by maximization of mutual information. *IEEE Trans Med Imaging*. 1997;16(2):187-198.
18. Wells WM, Viola P, Atsumi H, Nakajima S, Kikinis R. Multi-modal volume registration by maximization of mutual information. *Med Image Anal*. 1996;1(1):35-51.
19. Luan H, Qi F, Xue Z, Chen L, Shen D. Multimodality image registration by maximization of quantitative–qualitative measure of mutual information. *Pattern Recognit*. 2008;41(1):285-298.
20. Razlighi QR, Kehtarnavaz N. Spatial mutual information as similarity measure for 3-D brain image registration. *IEEE J Transl Eng Health Med*. 2014;2.
21. Woo J, Stone M, Prince JL. Multimodal registration via mutual information incorporating geometric and spatial context. *IEEE Trans Image Process Publ IEEE Signal Process Soc*. 2015;24(2):757-769.
22. Almukhtar A, Ju X, Khambay B, McDonald J, Ayoub A. Comparison of the accuracy of voxel based registration and surface based registration for 3D assessment of surgical change following orthognathic surgery. *PloS One*. 2014;9(4):e93402.
23. Dale AM, Fischl B, Sereno MI. Cortical surface-based analysis. I. Segmentation and surface reconstruction. *NeuroImage*. 1999;9(2):179-194.
24. Hahn HK, Peitgen H-O. The skull stripping problem in MRI solved by a single 3D watershed transform. In: Delp SL, DiGoia AM, Jaramaz B, eds. *Medical Image Computing and Computer-Assisted Intervention – MICCAI 2000. Lecture Notes in Computer Science*. Berlin Heidelberg: Springer; 2000:134-143.
25. Holmes CJ, Hoge R, Collins L, Woods R, Toga AW, Evans AC. Enhancement of MR images using registration for signal averaging. *J Comput Assist Tomogr*. 1998;22(2):324-333.
26. De Almeida AN, Olivier A, Quesney F, Dubeau F, Savard G, Andermann F. Efficacy of and morbidity associated with stereoelectroencephalography using computerized tomography–or magnetic resonance imaging-guided electrode implantation. *J Neurosurg*. 2006;104(4):483-487.
27. Guenot M, Isnard J, Ryvlin P, et al. Neurophysiological monitoring for epilepsy surgery: the Talairach SEEG method. StereoElectroEncephaloGraphy. Indications, results, complications and therapeutic applications in a series of 100 consecutive cases. *Stereotact Funct Neurosurg*. 2001;77(1-4):29-32.
28. Mathon B, Clemenceau S, Hasboun D, et al. Safety profile of intracranial electrode implantation for video-EEG recordings in drug-resistant focal epilepsy. *J Neurol*. 2015;262(12):2699-2712.
29. Cardinale F, Cossu M, Castana L, et al. Stereoelectroencephalography: surgical methodology, safety, and stereotactic application accuracy in 500 procedures. *Neurosurgery*. 2013;72(3):353-366; discussion 366.
30. Mullin JP, Shriver M, Alomar S, et al. Is SEEG safe? A systematic review and meta-analysis of stereo-electroencephalography-related complications. *Epilepsia*. 2016;57(3):386-401.
31. Gonzalez-Martinez J, Mullin J, Vadera S, et al. Stereotactic placement of depth electrodes in medically intractable epilepsy. *J Neurosurg*. 2014;120(3):639-644.
32. Blauwblomme T, David O, Minotti L, et al. Prognostic value of insular lobe involvement in temporal lobe epilepsy: a stereoelectroencephalographic study. *Epilepsia*. 2013;54(9):1658-1667.
33. Bouthillier A, Surbeck W, Weil AG, Tayah T, Nguyen DK. The hybrid operculo-insular electrode: a new electrode for intracranial investigation of perisylvian/insular refractory epilepsy. *Neurosurgery*. 2012;70(6):1574-1580; discussion 1580.

Supplemental digital content *is available for this article at (www.operativeneurosurgery-online.com.).*

Acknowledgments

The authors thank Béatrice Scholtes for critical proofreading, Thierry Cecchin and Jonathan Guedes (Université de Lorraine, CNRS, Nancy) for their helpful data management/analysis and Eric Pozza (University Hospital of Nancy) for MR/CT data management.